Article

The Effects of Surfactant and Metal Ions on the Stability and Rheological Properties of Nanoemulsions Loaded with Gardenia Yellow Pigment

Li Gao [†] and Bin Li *

College of Food Science and Technology, Huazhong Agricultural University, Wuhan 430070, China; gaoli19980711@hbeu.edu.cn
* Correspondence: libinfood@mail.hzau.edu.cn; Tel.: +86-27-63730040; Fax: +86-27-87288636
† Current Institution: College of Life Science and Technology, Hubei Engineering University, Xiaogan 432000, China.

Abstract: The present work reports the preparation of gardenia yellow pigment containing paraffin oil nanoemulsions stabilized by Span80 and Tween80. The preparation of the required nanoemulsions was optimized by testing different conditions, such as varying the hydrophilic–lipophilic balance (*HLB*), the emulsifier concentration (EC), the oil–water ratio (OWR), and the temperature (T), as determined by the average droplet diameter (ADD) and polydispersity index (PDI). Our results indicated that a minimum ADD of 65.9 nm and PDI of 0.116 were obtained at an optimum *HLB* value of 6.0, EC of 10% (*w/w*), OWR of 2:1, and T of 40 °C. Both the steady-state and dynamic rheological parameters were further investigated, revealing that the emulsions exhibited pseudoplastic behaviors. The long-term stabilities of the nanoemulsions after the addition of inorganic salts were monitored by observing their visual appearances. It was found that the emulsions containing pure water or 0.1 M $CaCl_2$ and $AlCl_3$ became slightly separated, while the emulsions containing 0.1 M KCl and NaCl showed no separation after 30 days of storage at room T. This difference among different salts could be related to the number of valence electrons of their cations. The spatial electrostatic effects of the monovalent cationic (KCl and NaCl) and the nonionic surfactants were greater than the delamination/sedimentation forces of the system, which was better than the salt based on the cations with valences greater than one ($CaCl_2$ and $AlCl_3$). In conclusion, the present work illustrated the formation, rheological properties, and stability of water containing gardenia yellow pigment in paraffin oil nanoemulsions, which can be of great significance for the application of gardenia-yellow-pigment-based formulations.

Keywords: gardenia yellow pigment; nanoemulsion; hydrophilic–lipophilic balance; stability; rheology

1. Introduction

Gardenia yellow pigment (GYP), extracted from *Gardenia jasminoides* Ellis, is a rare natural water-soluble carotenoid consisting of crocin and crocetin [1]. Crocins are series derivatives of crocetin glycosides [2] and are considered as the main components of water-soluble carotenoid in gardenia yellow, which is also used as a natural colorant. Moreover, it has been used as a natural food pigment for a long time, mainly for candy, noodles, jelly, and colored juice [3]. Crocetin, a type of carotenoid, contains a short carbon chain and carboxyl groups at both ends of the carbon chain [4]. It is an aglycone of crocin found in the fruit of gardenia [5] and is used as a traditional herbal medicine [4]. Crocetin has many obvious effects in the treatment of diseases, such as cancer, sleep disturbances, and atherosclerosis [2]. Crocetin and crocins have received much attention in recent years because of their health benefits and medical attributes, including their antioxidant properties, anti-inflammatory properties, and their ability to reduce body fatigue and

alleviate depression [5]. In light of the preceding discussion, gardenia yellow pigment-rich foods are regarded as beneficial for consumers' health.

Due to the coexistence of gardenoside, the gardenia yellow pigment easily fades and turns green when used as a food additive [6]. Gardenia yellow has been widely used as a natural pigment, but commercial gardenia yellow contains gardenoside, which may have negative effects [7]. Hence, it is crucial to prevent gardenia yellow from fading. A W/O nanoemulsion might be an effective way to overcome the stability-related limitations of gardenia yellow.

Nanoemulsions are emulsions with droplet sizes in the range of 50–500 nm that are optically transparent and exhibit high kinetic stability [8]. The two main types of nanoemulsions are oil-in-water (O/W) emulsions (which are oil phases dispersed in continuous aqueous phases), and water-in-oil (W/O) emulsions (which are water phases dispersed in continuous oil phases) [9]. These emulsions can be stabilized by the interfacial layer of the emulsifier and co-emulsifier [10–12]. The instability mechanisms of the nanoemulsions in various breakdown processes are mainly Ostwald ripening, coalescence, and flocculation [13]. The emulsifier composition, droplet size, and surface charge are directly related to the stability of the nanoemulsion. Nanoemulsions are gaining increasing attention due to their wide applications in the pharmaceutical, cosmetic, and food industries [14]. They have significant effects on the antioxidant activities of different bioactive compounds such as flavanols, resveratrol, and green tea polyphenols [15]. The W/O nanoemulsions' combination of nonionic emulsifiers can encapsulate bioactive compounds to protect and increase their properties, including stability, solubility, and antioxidativity [15].

Liquid paraffin or mineral oil is a highly refined petroleum derivative composed of saturated hydrocarbons and is widely used as an oral laxative in Lesotho [16,17]. This oil protects against constipation and encopresis, which may be attributed to its tolerability and fewer side effects [18]. Studies have shown that it is good for the skin and development of babies, as well as for mothers with depression [19]. Moreover, it has been used in lip care cosmetics and skin for decades due to its wide range of viscosity options, high protection and cleaning properties, and excellent skin tolerance. Compared with vegetable oils, paraffin oils are nonallergenic because they are very stable and do not easily oxidize or become rancid. They have a long history of safe use, which has been confirmed by clinical and epidemiological geological data [20]. Therefore, a liquid-paraffin-based nanoemulsion can be better utilized in cosmetics and medical applications.

In the present study, water containing gardenia yellow pigment in paraffin oil nanoemulsions was prepared and stabilized by a combination of Span80 and Tween80 surfactants. The main objective of the present study was to evaluate the stability of the emulsions formed at the optimum operating condition and to study the effects of the preparation parameters, e.g., the hydrophilic-lipophilic balance (*HLB*), the surfactant concentration, the oil-water ratio (OWR), the temperature (T), and the presence of inorganic salts on the stability of these emulsions. Furthermore, orthogonal and laser diffraction measurements were conducted to minimize the average droplet diameter (ADD) and polydispersity index (PDI) in order to select the most stable emulsion system for loading the hydrophilic gardenia yellow pigment.

2. Experimental Section

2.1. Materials

Crocin standard (98% content) was purchased from the Institute for the Verification of Pharmaceutical and Biological Products (Beijing, China). Liquid paraffin, Span80 and Tween80 surfactants, anhydrous calcium chloride, sodium chloride, potassium chloride, and aluminum chloride were obtained from Sinopharm Group Chemical Reagent Co., Ltd. (Shanghai, China) and were of analytical grade. Deionized water (Ultrapure, Thermo Fisher, Shanghai, China) was used in all the experiments.

2.2. Methods

2.2.1. Preparation of the Emulsions

The nanoemulsions were prepared using deionized water as the dispersed phase and paraffin oil as the continuous phase. First, the Tween80 and Span80 surfactants with different concentrations (4, 6, 8, 10, 12, 14, 16, 18, 20, and 30 wt%) at the required *HLB* values (4.5, 5, 5.5, 6, 6.5, and 7.0) were dispersed in liquid paraffin as the oil phase. The mixture was then heated to 50 °C for 30 min in a water bath. After cooling to room T (20–25 °C), the oil phase was stirred at 1000 rpm for 10 min (20 °C) using magnetic stirring, and the aqueous phase was added to the oil phase dropwise to form an emulsion in a 250-mL conical flask that contained gardenia yellow pigment (1.6 g) and NaCl solution (0.8 g) with the concentrations of 0.1 mg/mL and 0.1 mol/L, respectively. The addition was carried out in such a way that all of the water phase was added at a rate of 2 drops/s. The magnetic stirring was continued for an additional time at 2000 rpm at 40 °C. Once the stirring was complete, a white nanoemulsion was obtained.

2.2.2. Selection of *HLB* Values

To obtain a stable emulsion system, Span80 (*HLB*: 4.3) and Tween80 (*HLB*: 15.0) were mixed at the desired ratio to obtain *HLB* values in the 4.5–7.0 range (e.g., 4.5, 5, 5.5, 6, 6.5, and 7.0). The required *HLB* values of the oil phases were calculated according to the Griffin method, expressed as follows [21]:

$$HLB_{AB} = \frac{W_A \times HLB_A + W_B \times HLB_B}{W_A + W_B} \tag{1}$$

where HLB_{AB} is the *HLB* of the mixed surfactants *A* and *B*; HLB_A and HLB_B are the *HLB* values of surfactants *A* and *B*, respectively; and W_A and W_B are the weight percentages of *A* and *B*, respectively.

2.2.3. Optimization of the Preparation Conditions

In this study, W/O nanoemulsions were prepared by a low-energy emulsification method using the ADD and PDI as the evaluation criteria. Based on previous work [22], we first selected the *HLB* values (4.5, 5, 5.5, 6, 6.5, and 7.0), emulsifier concentrations (EC) (4, 6, 8, 10, 12, 14, 16, 18, 20, and 30 wt%), OWR (4:1, 3.5:1, 3:1, 2.5:1, 2:1, and 1:1 (*w/w*)), preparation T (30, 40, 50, 60, and 70 °C), and stirring times (20, 30, 40, 50, and 60 min) to perform a single factor test.

2.2.4. Optimization of the Formulas

Based on the examination of the single factors of the preparation conditions, we designed an L9 (34) orthogonal test to obtain the optimal formula composition by range analysis.

2.2.5. Determination of the Droplet Size and PDI

The ADD and PDI were determined using a laser particle size analyzer (Malvern Instruments, Malvern, UK). The samples were diluted in paraffin oil 1000 times (10 μL/10 mL) and stirred for 10 min at 1000 rpm using a vortex oscillator (Beijing United Keyi Technology Co., Ltd., MX-F, Beijing, China). After 12 h, the measurements were performed at 25 ± 2 °C and repeated in triplicate. The refractive index of the dispersed phase (deionized water) was 1.333 and that of the continuous phase (liquid paraffin) was 1.467.

2.2.6. Rheological Analysis

Rheological measurements were conducted using an AR2000ex rheometer (TA Instruments, New Castle, PA, USA) with a parallel plate (diameter 40 mm, gap 1.0 mm). Continuous flow tests were carried out. The continuous ramp step was selected as the test type, and the shear rate ranged from 0 to 120 s^{-1} within 2 min. Strain scanning measurements were performed in the range of 0.01 to 100% at the frequency of 1 rad/s to

obtain the elastic (G′) and loss (G″) moduli and compare the rheological parameters of different emulsions.

2.2.7. Long-Term Stability

Using the droplet size as the criterion, we evaluated the long-term stability of the W/O nanoemulsions prepared under the optimum conditions. The samples were sealed at room T for up to 30 days, and the particle sizes were measured at different time intervals.

2.2.8. Statistical Analysis

All the experiments were performed three times, and the data were expressed as mean ± SD (standard deviation). The single factor experimental data and statistical analysis were processed using Microsoft Excel 2007, and the orthogonal design and results were processed using the DPS v7.05 software.

3. Results and Discussion

3.1. Influence of the HLB Value

The *HLB* value is a useful parameter for selecting a nonionic surfactant, which affects the size distribution and particle size formation of a stable nanoemulsion. The PDI was used to investigate the dispersibility of the nanoemulsion, with a smaller value indicating better dispersion. Typically, emulsifiers with lower *HLB* values (<7.0) are suitable for the fabrication of W/O emulsions, whereas emulsifiers with higher *HLB* values (>7.0) are suitable for the preparations of O/W emulsions [23]. To obtain the required *HLB* value, Span80 and Tween80 were mixed at the desired ratios to obtain *HLB* values in the range of 4.5–7.0 (4.5, 5.0, 5.5, 6.0, 6.5, and 7.0).

As shown in Figure 1, when the *HLB* values increased from 4.5 to 6.0, the droplet size decreased from 129.33 to 89.24 nm. At lower *HLB* values, the mass fraction of Span80 was higher than that of Tween80, leading to the increased hydrophobicity of the mixed surfactant system, which could form a weak packing of the emulsifier molecules around the interface because of the imbalance between the hydrophobicity and hydrophilicity.
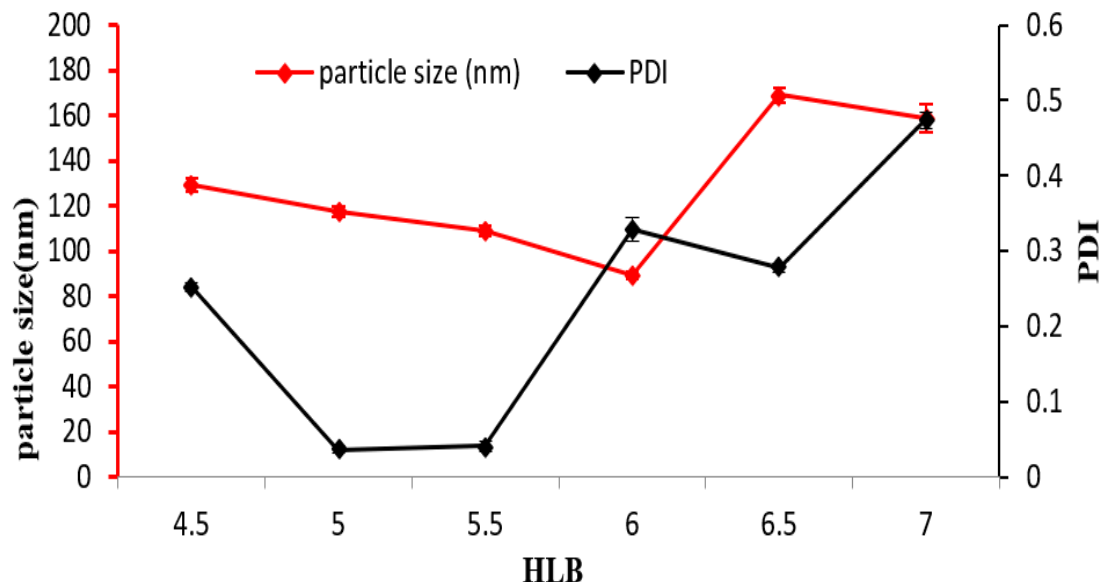

Figure 1. Effects of *HLB* on the stability of the emulsions.

However, due to the higher interfacial molecular area of Tween80 (Tween80: 2.48 nm^2; Span80: 0.46 nm^2), as the *HLB* values increased from 6.5 to 7.0, the droplet sizes did not significantly decrease. These results demonstrated that Tween80 and Span80 were in a saturated state on the droplet interface at an *HLB* of 6. At higher *HLB* values, excess

Tween80 molecules were present and occupied the largest active sites, which led to a lack of further reduction in the droplet size for *HLB* values greater than 6.0 [24,25]. The minimum particle size and PDI were found at the *HLB* values of 5.0 and 6.0, respectively. Therefore, the *HLB* values in the 5.0–6.0 range were selected for further experiments.

3.2. Influence of EC

The EC was varied in the 4–30 wt% range at a fixed *HLB* of 5.0. According to the surface tension theory, emulsification occurs by reducing the interfacial tension between the oil and water phases. However, an examination of the data presented in Figure 2 shows that there were no significant differences between the results obtained for the ECs of 4 and 6 wt%. The nanoemulsion gradually became layered below 6 wt% because here the concentration of emulsifier was not sufficient to decrease the interfacial tension, which led to the coalescence of aqueous droplets. At the fraction of 16 wt%, the prepared emulsion was translucent, whereas at a higher fraction (>16 wt%), the emulsion was more turbid. These results indicate that, after the critical micelle concentration was reached, the interfacial tension was not changed by the higher concentration of the surfactant [26].
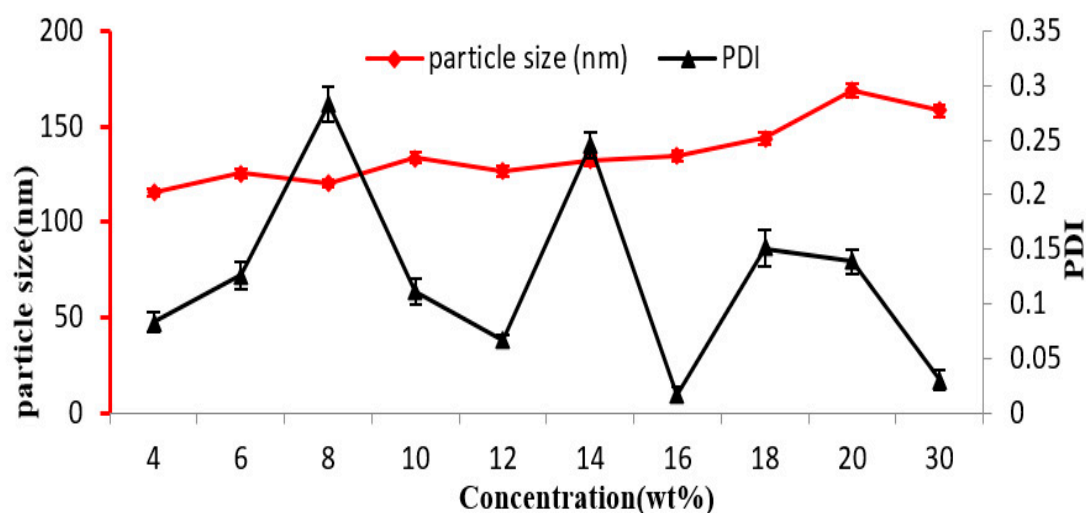

Figure 2. Effect of EC on the stability of the emulsions.

Furthermore, an increase in the EC resulted in a decrease in the PDI. As the emulsifier fraction increased from 8 to 16 wt%, the PDI decreased from 0.283 to 0.017, demonstrating that the formulations prepared at low mass fractions were unstable [14].

3.3. Influence of the Oil–Water Ratio (OWR)

The oil–water mass ratio will affect the viscosity of the system and the stability of the emulsion. The oil–water mass ratio was varied in the range from 1:1 to 4:1 at a fixed *HLB* of 5 and surfactant concentration of 12% (*w/w*). As shown in Figure 3, it can be observed that droplet size decreased from 154.0 nm to 124.0 nm on increasing ratios from 1:1 to 4:1 and the PDI exhibited no big difference. A higher ratio resulted in smaller droplet size due to decrease in the viscosity of emulsion, and small viscosity is beneficial to the dispersion of droplets [27]. The emulsions prepared at a ratio of 1:1 to 1.5:1 were found to be unstable after 24 h of storage at room temperature, whereas the emulsions prepared at a ratio of 2:1 to 4:1 were more stable under the same conditions, respectively, and the most stable emulsion appeared at the 3:1 oil–water mass ratio. It indicated that emulsions of a higher oil–water ratio reduced the viscosity of the system, leading to dispersing the droplets sufficiently, which could make the droplet size smaller.
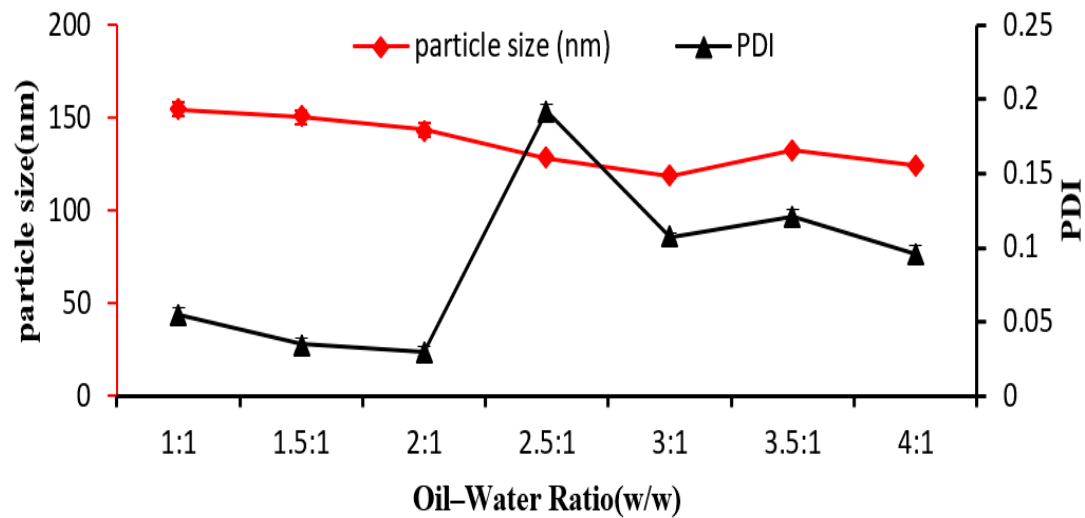
Figure 3. Effects of different OWRs on stability of the emulsions.

However, under a smaller oil and water ratio, the water content was relatively excessive and additional water led to parts of emulsifiers in the system dispersed in it, which resulted in insufficient emulsification of liquid paraffin wax, so the particle size of the emulsion became larger.

3.4. Influence of T

To study the effects of T, the T was varied in the 30–70 °C range at a fixed *HLB* of 8.0, EC of 12 wt%, and OWR of 3:1. The T had a significant effect on the droplet size. As shown in Figure 4, upon increasing the T from 30 to 70 °C, the droplet size increased from 119.36 to 189.08 nm, and the PDI also increased from 0.015 to 0.035. This indicated that a higher T influenced the evaporation rate of the organic solvent [28], and the gradual dehydration of emulsifier at the oil–water interface gave rise to the increase in interfacial tension, which promoted the coalescence of liquid droplets [29].
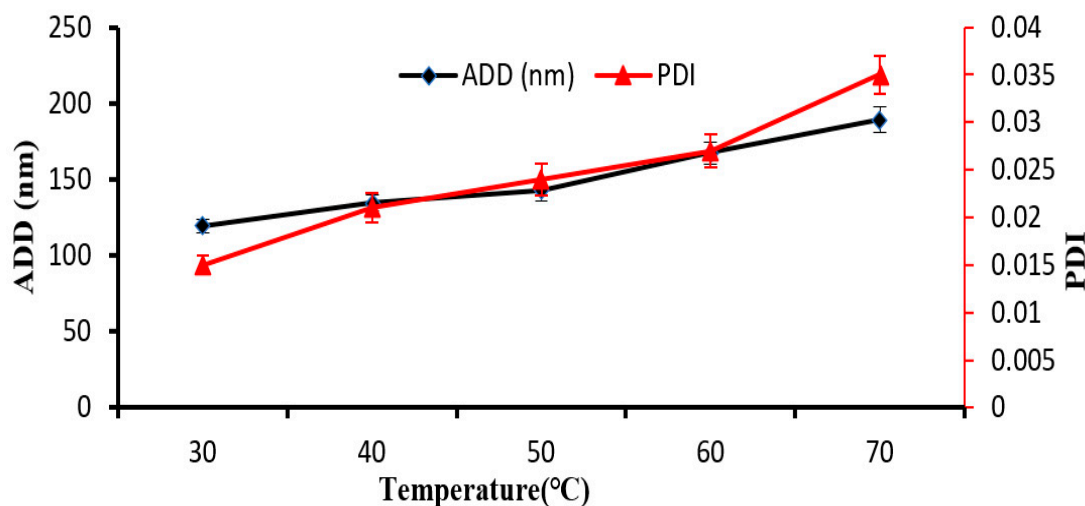

Figure 4. Effect of preparation T on stability of the emulsions.

3.5. Orthogonal Experiments Design

Various methods, such as the single factor method and the response surface method [30], were used to optimize the experimental conditions. In the present study, to reduce the experimental time, orthogonal experiments, which can be used to assess the importance

of each factor and determine the ideal values, were performed for the optimization of the preparation conditions of the W/O emulsions [31,32]. In the preparation process of the W/O emulsions, the preparation conditions were optimized by L9 (34) orthogonal experiments using the ADD and the PDI as the assessment indices. The *HLB* value (A), EC (B), OWR (C), and preparation T (PT (D)) were selected as the experimental factors. Each factor was designed with three levels, and the factors and levels of the orthogonal tests are listed in Table 1, with the results shown in Table 2.

Table 1. Factors and levels of Orthogonal experiment.

	Factor			
Level	*HLB*	**EC (wt%)**	**OWR (*w/w*)**	**T (°C)**
	A	**B**	**C**	**D**
1	5.0	10	2:1	40
2	5.5	12	3:1	50
3	6.0	16	4:1	60

Table 2. Results of the Orthogonal experiment.

Run		*HLB*	EC (wt%)	OWR (*w/w*)	T (°C)	ADD (nm)	PDI
		A	**B**	**C**	**D**		
1		1	1	1	1	120.432	0.032
2		1	2	2	2	141.105	0.172
3		1	3	3	3	189.306	0.148
4		2	1	2	3	130.423	0.152
5		2	2	3	1	117.406	0.082
6		2	3	1	2	141.323	0.011
7		3	1	3	2	99.207	0.225
8		3	2	1	3	94.104	0.573
9		3	3	2	1	104.413	0.204
	k_1	150.28	116.69	118.62	114.08		
ADD	k_2	129.72	117.54	125.31	127.21		
	k_3	99.24	145.01	135.31	137.94		
	R	51.04	28.33	16.69	23.86		
		order of importance A > B > D > C					
		optimal level $A_3B_1D_1C_1$					
	k_1	0.12	0.14	0.21	0.11		
PDI	k_2	0.08	0.28	0.14	0.14		
	k_3	0.33	0.12	0.15	0.29		
	R	0.25	0.16	0.06	0.19		
		order of importance A > D > B > C					
		optimal level $A_2D_1B_3C_2$					

As shown in Table 2, the PDI values of runs 7, 8, and 9 were 0.225, 0.573, and 0.204, respectively, while those of the other runs were less than 0.2. The ADD values of runs 7 and 8 were 99.207 and 94.104 nm, respectively, while those of the other runs exceeded 100 nm. The results of the range analysis used to determine the optimal levels of the factors are shown in Table 2. The K/k value for each level was the average of three ADD values and the polydispersity index (PDI), as shown in Table 2. By comparing different K/k values, the optimal level of factors for the preparation of the W/O nanoemulsions could be identified. In this work, the minimum K/k value was better for the optimal level. The difference between the maximum and minimum K/k values is represented by the range value (R), which reflects the detrimental effects of the level on the ADD and PDI. The most important factor was obtained when R was maximal, and the order of importance was A > B > D > C and A > D > B > C for the ADD and PDI, respectively [33,34].

Considering the practicability of the W/O emulsions, the ADD was the most important factor for the formulation selection. The factors influencing the ADD were in the order of *HLB* value > EC > emulsification T > OWR. The final optimal preparation factors were a *HLB* of 6.0, EC of 10 wt%, OWR of 2:1, and emulsification T of 40 °C.

However, the optimal combination was not listed in the nine runs (Table 2), and three additional validation experiments showed that the ADD and the PDI were 45.15 nm and 0.25, respectively, under the optimal preparation conditions (Table 3). These values were smaller than those obtained in any of the nine runs, which confirmed the reliability of the model prediction by the array.

Table 3. Confirmatory experiment.

Factor	*HLB*	EC (*wt%*)	OWR (*w/w*)	T (°C)
condition	6	10	2:1	40
times	once	second	third	mean
ADD (nm)	73.17	65.91	65.83	45.15
PDI	0.27	0.12	0.3	0.25

Notably, as shown in Figure 5, the laser diffraction measurements exhibited that the W/O nanoemulsion particle size distribution was relatively uniform, and the width was substantially unchanged. This indicated that the adjustment of the proportions of the added materials could significantly reduce the interfacial tension of the water and oil, such that the Ostwald ripening rate was weak, physical changes such as Brownian motion could be resisted, and the nanoemulsion stability could be improved. The more stable the emulsion system, the more obvious the protective effect of the gardenia yellow pigment.
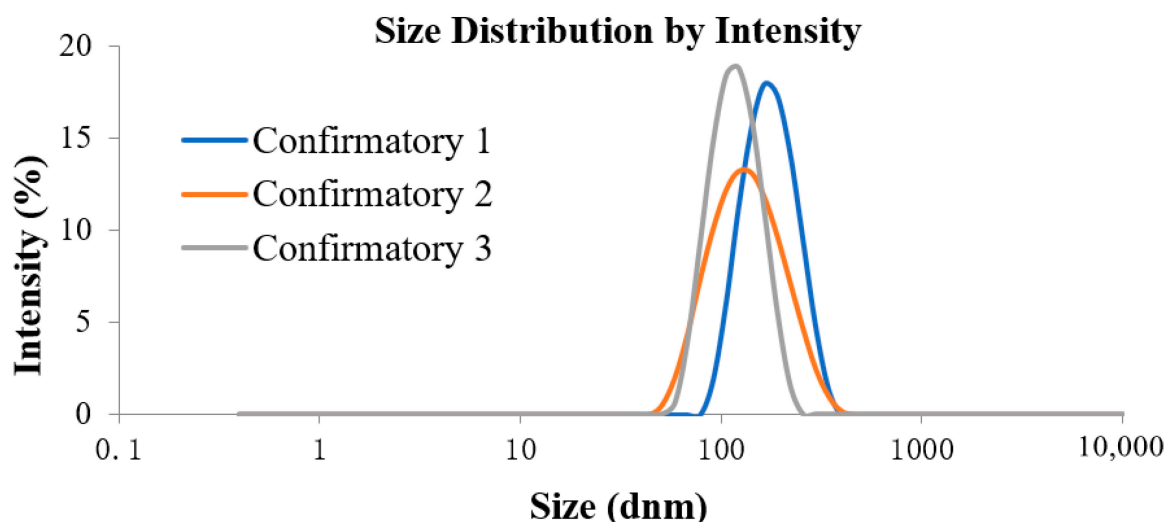

Figure 5. Particle size distribution of nanoemulsion with the confirmatory experiment.

3.6. Rheology

3.6.1. Shear Flow Tests

Research has revealed that high emulsion viscosity is conducive to its stability [35]. As shown in Figure 6a, the viscosity decreased significantly with the increase in the shear rate. At higher shear rates, the viscosity tended to be almost constant, indicating that the W/O nanoemulsion was a pseudoplastic fluid with shear thinning behavior [36]. This was due to the higher shear strain leading to more obvious elongation, deformation, and network fracture of the nanoemulsion droplets [37].
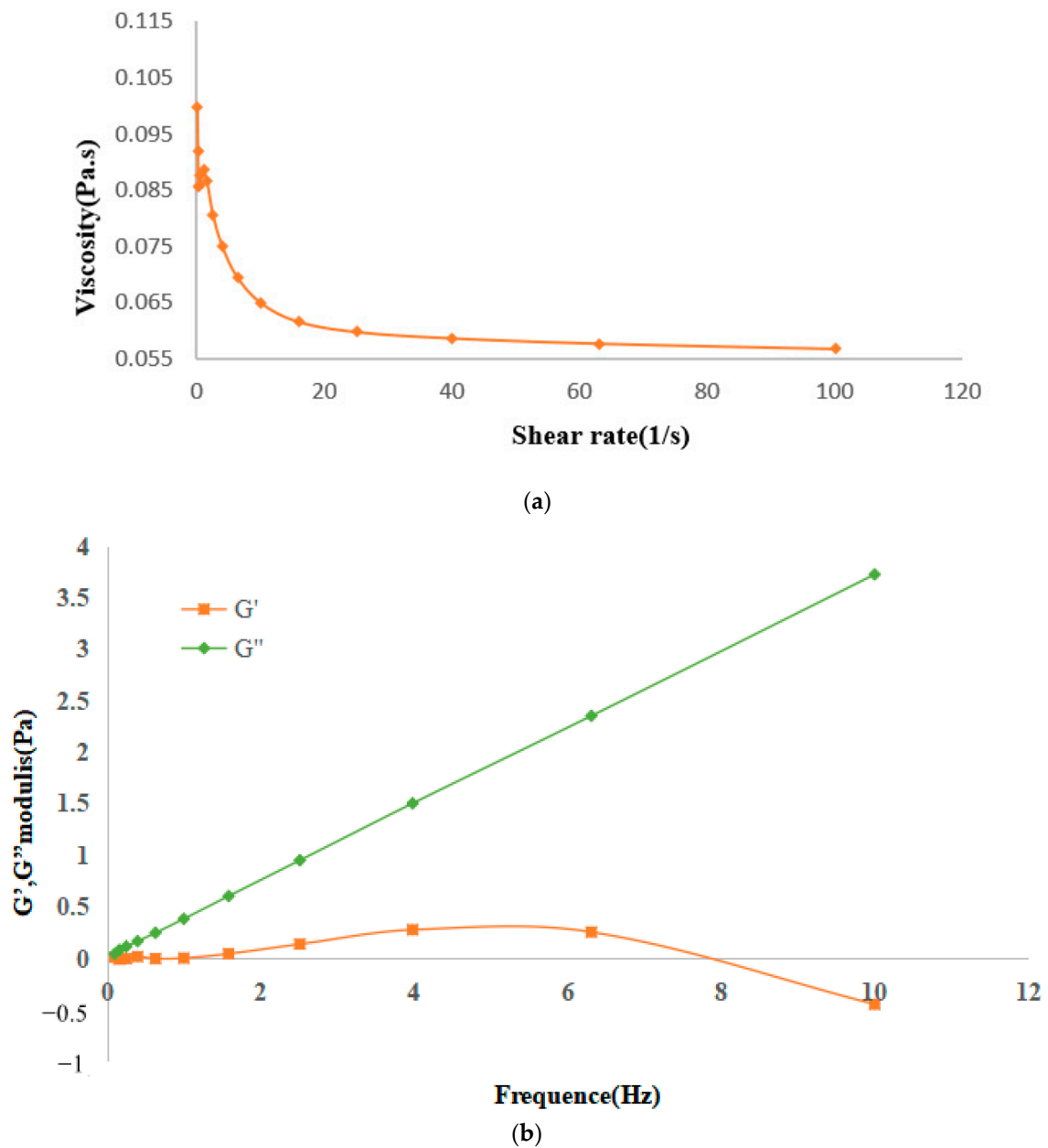
(a)

(b)

Figure 6. The relationship between viscosity and shear rate for optimal nanoemulsion (**a**); The change of elastic modulus and viscous modulus with frequency (**b**).

3.6.2. Oscillation Strain Sweep

Oscillation strain sweep tests were conducted to characterize the structural strengths of the emulsions in the linear viscoelastic region. Figure 6b shows the frequency dependence of the dynamic modulus. The storage modulus (G′) is a measure of the energy stored elastically during an oscillation cycle, whereas the loss modulus (G″) is a measure of the energy dissipated by the viscous flow during the oscillation. The G′ modulus was negligible compared to the G″ for the nanoemulsions with 10% (*w*/*w*) surfactant concentrations; thus, the emulsions exhibited a predominant viscous behavior.

However, as can be seen from Figure 7, when the surfactant concentration was 20% and 24% (*w*/*w*), the G′ value of the two emulsions was about twice as high as that of G″, indicating that the emulsion had a certain elasticity. The modulus of elasticity depended on the types of interaction forces between the droplets and their nearest neighbors—attractive or repulsive [38,39]. The change from a predominantly viscous to a predominantly elastic

response was affected by the ratio of the adsorption thickness of the surfactant to the droplet radius R [39].
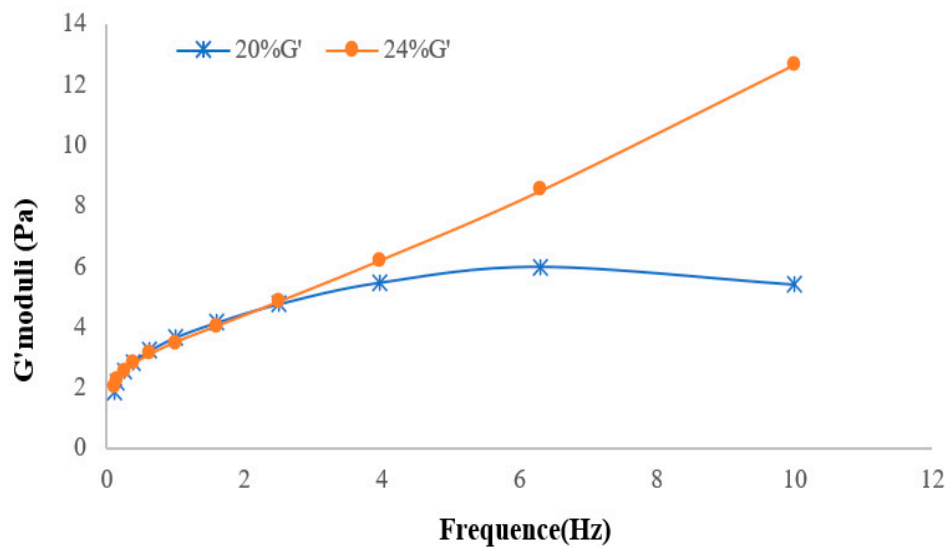
(**a**)
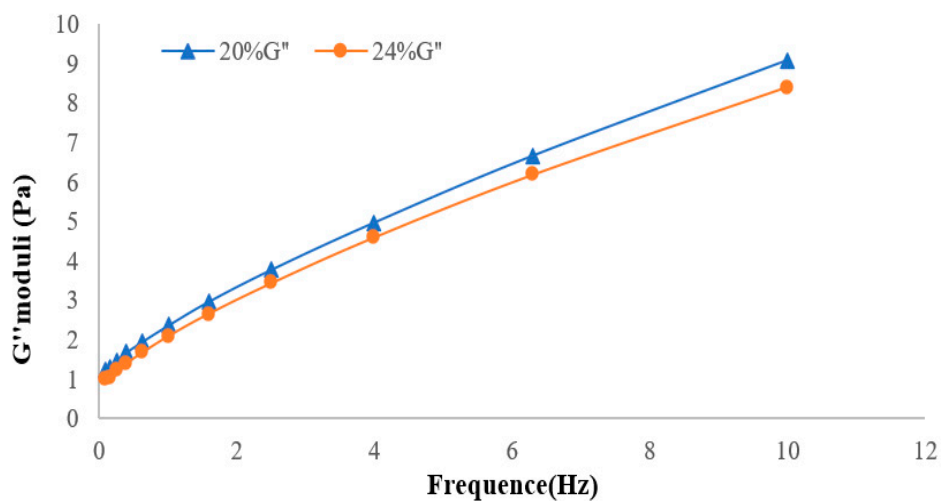
(**b**)

Figure 7. Dynamic (**a**,**b**) rheological analyses of W/O emulsions with different ECs. (**a**) dynamic rheological analysis of W/O emulsions with different ECs and elastic moduli G′, and (**b**) dynamic rheological analysis of W/O emulsions with different ECs and loss moduli G″.

3.7. Stability Evaluation of the Emulsions

In this study, the effects of different chloride salts (sodium, potassium, aluminum, and calcium) at 0.1 M concentrations on the long-term stability of the W/O nanoemulsions were examined. As shown in Figure 8, the addition of chloride salts in the aqueous phase had little effect on the initial ADD and did not result in significant differences in the stability compared to the systems with no added salt. This indicated that the EC was the main determinant of the initial particle size of the W/O nanoemulsions. As shown in Figure 9, after 30 days of observation at room T, the emulsions containing pure water or 0.1 M $CaCl_2$ and $AlCl_3$ slightly separated, whereas the emulsions containing 0.1 M KCl and NaCl did

not show any separation until 30 days at room T. This difference was related to the number of valence electrons of the cations of these salts.
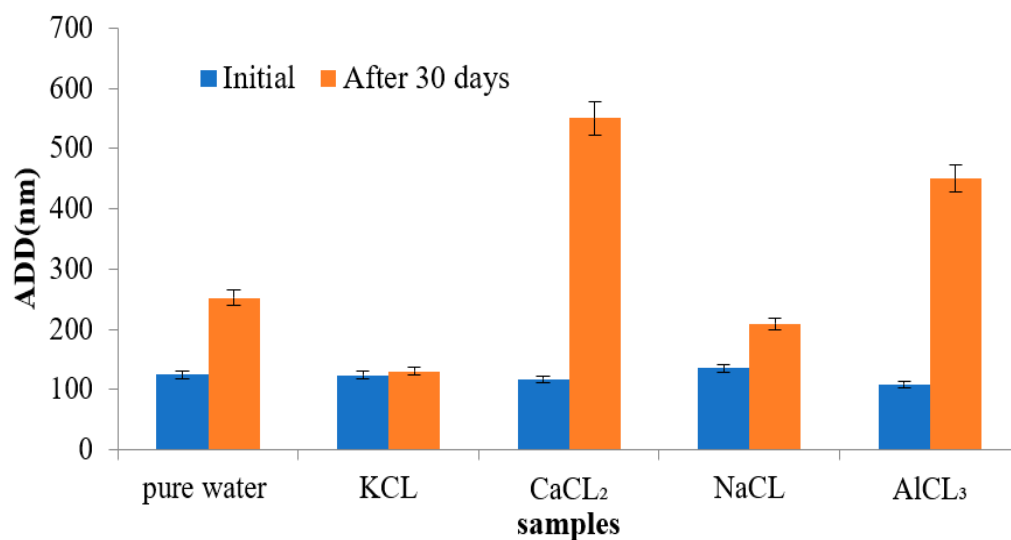

Figure 8. Long-term stability of pure water nanoemulsions and nanoemulsions with 0.1 M salts.
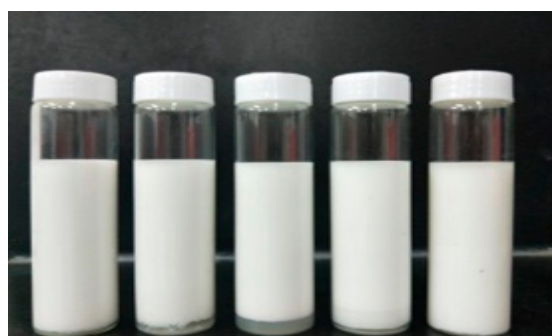

Figure 9. Appearance of pure water nanoemulsions and nanoemulsions with 0.1 M salts after storage for 30 days. The type of salt from left to right are pure water, AlCl$_3$, CaCl$_2$, NaCl, and KCl.

KCl and NaCl are ionic compounds, and upon addition to the water phase, these crystals dissociate into Na$^+$, K$^+$, and Cl$^-$ ions in water. It is well known that the emulsification process includes the break-up of droplets and the re-coalescence of the newly formed droplets. The investigations by Jafari et al. [40]. showed that the reduction in the re-coalescence was stronger than the enhancement of the droplet disruption. According to Tadros [41], the stability of the oil–water interface depends on the electrostatic or spatial repulsion interactions. Therefore, when KCl and NaCl dissociated into ions in water, due to the reduced re-coalescence, these ions gave rise to repulsive interactions in the droplets that could improve the stability of the oil–water interface. This conclusion agrees with the results reported by Scherze et al. [42].

For the effect of CaCl$_2$ and AlCl$_3$ on the nanoemulsion stability, it was suggested that a reduction in the attractive force between the water droplets due to the addition of the electrolytes in the aqueous phase increased the W/O emulsion stability with respect to the coalescence. Consequently, the attractive forces were minimized by matching the refractive indices and/or the dielectric constants of the two phases. As the electrolyte concentration increased, the refractive index of the aqueous phase increased, and the ionization constant decreased [43]. Thus, the addition of calcium and aluminum salts decreased the attractive forces, leading to the reduced frequency of collisions between the water droplets, improving the stability with respect to the coalescence of the W/O emulsions, and leading to their sedimentation.

The above results demonstrated that the spatial electrostatic effects of the monovalent cationic (KCl and NaCl) and the nonionic surfactants were greater than the delamination/sedimentation forces of the system, providing effective resistance to the destabilizing processes, such as Ostwald ripening, coalescence, and flocculation. Thus, the emulsions with NaCl and KCl had small particle sizes, narrow particle size distributions, and better long-term stability, whereas the nanoemulsions with salts based on cations with valences greater than one ($CaCl_2$ and $AlCl_3$) showed the opposite effects.

4. Conclusions

In this work, gardenia-yellow-pigment-based W/O nanoemulsions were produced, and the effect of the surfactant and metal ions on the nanoemulsions was studied. The optimal W/O nanoemulsions' preparation parameters were defined by single factor experiments and orthogonal tests, including the hydrophilic–lipophilic balance (*HLB*) value (6), the emulsifier concentration (10%), the oil–water ratio (2:1), and the preparation temperature (40 °C). The experimental analysis showed that the W/O nanoemulsions were shear thinning pseudoplastic fluids, and the rheology of the W/O nanoemulsions changed from viscosity to elasticity by adding the appropriate concentration of surfactant. In particular, the stability of the nanoemulsion was improved by electrostatic and spatial exclusion after NaCl and KCl addition, whereas the instability mechanism after $CaCl_2$ and $AlCl_3$ addition resulted in coalescence and sedimentation. This preliminary study provides new insight into the design of new generation nanoemulsions containing gardenia yellow pigment for health promotion. The outcomes can be considered as the beginning, requiring further research focused on gardenia yellow pigment for commercial usage.

Abbreviations

ADD	average droplet diameter
EC	emulsifier concentration
HLB	hydrophilic–lipophilic balance
O/W	oil-in-water
OWR	oil–water ratio
PDI	polydispersity index
PT	preparation T
SD	standard deviation
T	temperature
W/O	water-in-oil

References

1. Wu, J.; Zhang, J.; Yu, X.; Shu, Y.; Zhang, S.; Zhang, Y. Extraction optimization by using response surface methodology and purification of yellow pigment from *Gardenia jasminoides* var. *radicans Makikno. Food Sci. Nutitionr.* **2020**, *9*, 822–832. [CrossRef] [PubMed]
2. Li, N.; Fan, M.; Li, Y.; Qian, H.; Zhang, H.; Qi, X.; Wang, L. Stability assessment of crocetin and crocetin derivatives in *Gardenia* yellow pigment and *Gardenia* fruit pomace in presence of different cooking methods. *Food Chem.* **2019**, *312*, 126031. [CrossRef] [PubMed]
3. Shang, Y.; Zhang, Y.; Cao, H.; Ma, Y.; Wei, Z. Comparative study of chemical compositions and antioxidant activities of Zhizi fruit extracts from different regions. *Heliyon* **2019**, *5*, e02853. [CrossRef]
4. Mori, K.; Torii, H.; Fujimoto, S.; Jiang, X.; Ikeda, S.; Yotsukura, E.; Koh, S.; Kurihara, T.; Nishida, K.; Tsubota, K. The Effffect of Dietary Supplementation of Crocetin for Myopia Control in Children: A Randomized Clinical Trial. *J. Clin. Med.* **2019**, *8*, 1179. [CrossRef]
5. Umigaia, N.; Takedab, R.; Moric, A. Effffect of crocetin on quality of sleep: A randomized, double-blind, placebo controlled, crossover study. *Complement. Ther. Med.* **2018**, *41*, 4–51.
6. Chen, L.; Li, M.; Yang, Z.; Tao, W.; Wang, P.; Tian, X.; Li, X.; Wang, W. *Gardenia jasminoides* Ellis: Ethnopharmacology, phytochemistry, and pharmacological and industrial applications of an important traditional Chinese medicine. *J. Ethnopharmacol.* **2020**, *257*, 112829. [CrossRef]
7. Inoue, K.; Tanada, C.; Nishikawa, H.; Matsuda, S.; Tada, A.; Ito, Y.; Min, J.Z.; Todoroki, K.; Sugimoto, N.; Toyo'oka, T.; et al. Evaluation of gardenia yellow using crocetin from alkaline hydrolysis based on ultra high performance liquid chromatography and high-speed countercurrent chromatography. *J. Sep. Sci.* **2014**, *37*, 3619–3624. [CrossRef]
8. Mandal, A.; Bera, A. Surfactant Stabilized nanoemulsion: Characterization and Application in Enhanced Oil Recovery. *World Acad. Sci. Eng. Technol.* **2012**, *6*, 537–542.
9. Rai, V.K.; Mishra, N.; Yadav, K.S.; Yadav, N.P. Nanoemulsion as Pharmaceutical Carrier for Dermal and Transdermal Drug Delivery: Formulation Development, Stability Issues, Basic Considerations and Applications. *J. Control. Release* **2018**, *270*, 203–225. [CrossRef]
10. Sood, S.; Jain, K.; Gowthamarajan, K. Optimization of Curcumin nanoemulsion for Intranasal Delivery Using Design of Experiment and Its Toxicity Assessment. *Colloids Surf. B Biointerfaces* **2014**, *113*, 330–337. [CrossRef]
11. Gorain, B.; Choudhury, H.; Kundu, A.; Sarkar, L.; Karmakar, S.; Jaisankar, P.; Pal, T.K. nanoemulsion Strategy for Olmesartan Medoxomil Improves Oral Absorption and Extended Antihypertensive Activity in Hypertensive Rats. *Colloids Surf. B Biointerfaces* **2014**, *115*, 286–294. [CrossRef] [PubMed]
12. Zhao, L.; Wei, Y.; Huang, Y.; He, B.; Zhou, Y.; Fu, J. Nanoemulsion Improves the Oral Bioavailability of Baicalin in Rats: In Vitro and In Vivo Evaluation. *Int. J. Nanomed.* **2013**, *8*, 3769–3779. [CrossRef] [PubMed]
13. Solans, C.; Izquierdo, P.; Nolla, J.; Azemar, N.; Garciacelma, M.J. Nanoemulsions. *Curr. Opin. Colloid Interface Sci.* **2005**, *10*, 102–110. [CrossRef]
14. Carpenter, J.; Saharan, V.K. Ultrasonic assisted formation and stability of mustard oil in water nano–emulsion: Effect of process parameters and their optimization. *Ultrason. Sonochem.* **2017**, *35*, 422–430. [CrossRef] [PubMed]
15. Mohammadi, A.; Jafari, S.M.; Esfanjani, A.F.; Akhavan, S. Application of nanoencapsulated olive leaf extract in controlling the oxidative stability of soybean oil. *Food Chem.* **2016**, *190*, 513–519. [CrossRef]
16. Sharif, F.; Crushell, E.; O'Driscoll, K.; Bourke, B. Liquid paraffin: A reappraisal of its role in the treatment of constipation. *Arch. Dis. Child.* **2001**, *85*, 121–124. [CrossRef]
17. Williams, S.E.; Docherty, M.H. Constipation complication: Lung injury following inadvertent intravenous injection of liquid paraffin. *Case Rep.* **2016**, *2016*, bcr2015213685. [CrossRef]
18. Urganci, N.; Akyildiz, B.; Polat, T.B. A comparative study: The effificacy of liquid paraffin and lactulose in management of chronic functional constipation. *Pediatr. Int.* **2005**, *47*, 5–19. [CrossRef]
19. Vermén, M.; Verallo, R.; Stephanie, S.; Katalbas, J.P. Pangasinan1. *Curr. Allergy Asthma Rep.* **2016**, 16–51.
20. Chuberre, B.; Araviiskaia, E.; Bieber, T.; Barbaud, A. Mineral oils and waxes in cosmetics: An overview mainly based on the current European regulations and the safety profile of these compounds. *JEADV* **2019**, *33*, 5–14. [CrossRef]
21. Griffin, W.C. Calculation of *HLB* Values of Non-Ionic Surfactants. *Am. Perfum. Essent. Oil Rev.* **1955**, *65*, 26–29.
22. Zhang, D.; Song, X.; Liang, F.; Li, Z.; Liu, F. Stability and Phase Behavior of Acrylamide-Based Emulsions before and after Polymerization. *J. Phys. Chem. B* **2006**, *110*, 9079–9084. [CrossRef] [PubMed]
23. Li, C.; Mei, Z.; Liu, Q.; Wang, J.; Xu, J.; Sun, D. Formation and Properties of Paraffin Wax Submicron Emulsions Prepared by the Emulsion Inversion Point Method. *Colloids Surf. A Physicochem. Eng. Asp.* **2010**, *356*, 71–77. [CrossRef]
24. Liu, W.; Sun, D.; Li, C.; Liu, Q.; Xu, J. Formation and Stability of Paraffin Oil-in-Water nanoemulsions Prepared by the Emulsion Inversion Point Method. *J. Colloid Interface Sci.* **2006**, *303*, 557–563. [CrossRef]
25. Leong, T.S.H.; Wooster, T.J.; Kentish, S.E.; Ashokkumar, M. Minimising Oil Droplet Size Using Ultrasonic Emulsification. *Ultrason. Sonochem.* **2009**, *16*, 721–727. [CrossRef]
26. Rafati, H.; Coombes, A.G.A.; Adler, J.; Holland, J.; Davis, S.S. Protein-Loaded Poly(DL-lactide-co-glycolide) Microparticles for Oral Administration: Formulation, Structural and Release Characteristics. *J. Control. Release* **1997**, *43*, 89–102. [CrossRef]

27. Alayoubi, A.; Abufayyad, A.; Rawasqalaji, M.M.; Sylvester, P.W.; Nazzal, S. Effect of lipid viscosity and high-pressure homogenization on the physical stability of "Vitamin E" enriched emulsion. *Pharm. Dev. Technol.* **2014**, *20*, 555–561. [CrossRef]
28. Pandey, S.K.; Patel, D.K.; Thakur, R.; Mishra, D.P.; Maiti, P.; Haldar, C. Anti-Cancer Evaluation of Quercetin Embedded PLA Nanoparticles Synthesized by Emulsified Nanoprecipitation. *Int. J. Biol. Macromol.* **2015**, *75*, 521–529. [CrossRef]
29. McClements, D.J. *Food Emulsions: Principles, Practices, and Techniques*, 3rd ed.; CRC Press: Boca Raton, FL, USA, 2015.
30. Wei, Z.J.; Liao, A.M.; Zhang, H.X.; Liu, J.; Jiang, S.T. Optimization of Supercritical Carbon Dioxide Extraction of Silkworm Pupal Oil Applying the Response Surface Methodology. *Bioresour. Technol.* **2009**, *100*, 4214–4219. [CrossRef]
31. Xie, G.; Chen, Z.; Ramakrishna, S.; Liu, Y. Orthogonal Design Preparation of Phenolic Fiber by Melt Electrospinning. *J. Appl. Polym. Sci.* **2015**, *132*, 42574. [CrossRef]
32. Liu, M.; Cheng, Z.; Jin, Y.; Ru, X.; Ding, D.; Li, J. Optimization and Investigation of the Governing Parameters in Electrospinning the Home-Made Poly(L-lactide-co-ε-caprolactone-diOH). *J. Appl. Polym. Sci.* **2013**, *130*, 3600–3610. [CrossRef]
33. Vild, A.; Teixeira, S.; Kühn, K.; Cuniberti, G.; Sencadas, V. Orthogonal Experimental Design of Titanium Dioxide—Poly(methyl methacrylate) Electrospun Nanocomposite Membranes for Photocatalytic Applications. *J. Environ. Chem. Eng.* **2016**, *4*, 3151–3158. [CrossRef]
34. Alam, H.G.; Moghaddam, A.Z.; Omidkhah, M.R. The Influence of Process Parameters on Desulfurization of Mezino Coal by HNO_3/HCl Leaching. *Fuel Process. Technol.* **2009**, *90*, 1–7. [CrossRef]
35. Jafari, S.M.; Beheshti, P.; Assadpoor, E. Rheological behavior and stability of d-limonene emulsions made by a novel hydrocolloid (Angum gum) compared with Arabic gum. *J. Food Eng.* **2012**, *109*, 1–8. [CrossRef]
36. Gong, J.; Wang, L.; Wu, J.; Yuan, Y.; Mu, R.-J.; Du, Y.; Wu, C.; Pang, J. The rheological and physicochemical properties of a novel thermosensitive hydrogel based on konjac glucomannan/gum tragacanth. *LWT* **2019**, *100*, 271–277. [CrossRef]
37. Yildirim, M.; Sumnu, G.; Sahin, S. The effects of emulsifier type, phase ratio, and homogenization methods on stability of the double emulsion. *J. Dispers. Sci. Technol.* **2017**, *38*, 807–814. [CrossRef]
38. Sherman, P. Rheological Changes in Emulsions on Aging: III. At Very Low Rates of Shear. *J. Colloid Interface Sci.* **1967**, *24*, 107–114. [CrossRef]
39. Tadros, T.F. Fundamental Principles of Emulsion Rheology and Their Applications. *Colloids Surf. A Physicochem. Eng. Asp.* **1994**, *91*, 39–55. [CrossRef]
40. Jafari, S.M.; Assadpoor, E.; He, Y.; Bhandari, B. Re-Coalescence of Emulsion Droplets during High-Energy Emulsification. *Food Hydrocoll.* **2008**, *22*, 1191–1202. [CrossRef]
41. Tadros, T.F. Emulsion Formation, Stability, and Rheology. In *Emulsion Formation and Stability*; Tadros, T.F., Ed.; Wiley-VCH: Weinheim, Germany, 2013; pp. 1–75.
42. Scherze, I.; Knoth, A.; Muschiolik, G. Effect of Emulsification Method on the Properties of Lecithin-and PGPR-Stabilized Water-in-Oil-Emulsions. *J. Dispers. Sci. Technol.* **2006**, *27*, 427–434. [CrossRef]
43. Márquez, A.L.; Medrano, A.; Panizzolo, L.A.; Wagner, J.R. Effect of Calcium Salts and Surfactant Concentration on the Stability of Water-in-Oil (W/O) Emulsions Prepared with Polyglycerol Polyricinoleate. *J. Colloid Interface Sci.* **2010**, *341*, 101–108. [CrossRef] [PubMed]